Nuclear Physics B74 (1974) 211–236. North-Holland Publishing Company

QUASI THREE BODY e^+e^- ANNIHILATION

A.C. HIRSHFELD * and G. KRAMER
II. Institut für Theoretische Physik der Universität Hamburg

Received 4 January 1974

Abstract: We present the helicity formalism for e^+e^- annihilation into three-body and quasi-three-body final states. We derive expressions for the cross sections and angular distributions in the one-photon-exchange approximation. For the process $e^+e^- \to \rho\pi\pi$ we exhibit the results of calculations based on various low-lying exchanges and VMD assumptions for the form factors. When two of the final state particles resonate, our formalism allows us to study the reliability of the narrow-width approximation made in previous work, and to include certain interference effects previously neglected.

1. Introduction

Recently a series of experiments on e^+e^- annihilation into hadrons at center of mass energies up to 5 GeV have been performed at Orsay, Frascati and CEA [1]. In the near future we expect further interesting experimental results from the colliding beam facilities at SLAC and DESY: firstly of course because the energy range will be extended, but also because the higher luminosities of these machines will provide far more detailed information about the hadron final states in the energy region already covered.

It has been argued that a large part of the measured cross section can already be explained in this energy range just by the production of two-body and quasi-two-body final states and their subsequent decays [2]. The general formalism for such two-body production has recently been given [3]. The cross sections $e^+e^- \to h_1h_2$ are related to the electromagnetic form factors for $\gamma \to h^+h^-$ and transition form factors $\gamma \to h_1h_2$ in the time-like region; these correspond to three-point functions.

From the theoretical point of view the next case of interest would be the three-body or quasi-three-body production. One now relates the cross sections for $e^+e^- \to h_1h_2h_3$ to the four-point amplitudes $\gamma \to h_1h_2h_3$ which correspond by crossing to two-to-two scattering amplitudes. We develop here the appropriate formalism **. This can be of help, on the one hand, for analysing experimental

* Now at Universität Dortmund.

** The formalism for an arbitary number of particles in the final state is developed by Avram and Schiller [4].

data on three-body production. On the other hand it provides insight concerning the limitations inherent in the two-body interpretation of many-body data.

In the two-body description of many-body final states the resonances are necessarily treated in the zero-width approximation. The effect of symmetrization for decay products of resonances is also neglected. In a three-body treatment we can take into account the effects of the finite widths of the resonances, and the interference effects between different channels.

We derive here the relation between the measurable differential cross sections and the four-body helicity amplitudes in the one-photon approximation. As in the two-body case this approximation leads to certain well defined angular distributions.

The Adone results have shown that multi-meson final states are copiously produced [1]. We consider in this context the example of $\rho\pi\pi$ production as the simplest final state with non-trivial spin structure. Examination of the Frascati results on $e^+e^- \to \pi^+\pi^-\pi^+\pi^-$ [5] shows that, as one would expect, the $\rho^0\pi^+\pi^-$ configuration probably accounts for at least 80% of the four-pion final state. It is clear that from the energy dependence of the total cross section, which is all that has been studied up to now, it is difficult to gain reliable information concerning the production mechanism. In order to gain insight in this regard it will be necessary to investigate differential cross sections and angular distributions. In order to generate some feeling for these distributions we calculate the contributions of the low-lying resonances and particle pole exchanges in the various channels to the different amplitudes and cross sections. More ambitious theoretical approaches to the dynamics of e^+e^- annihilation which exist in the literature [6] are mainly concerned with more global properties, and/or asymptotic predictions.

Of course, an interesting problem concerns the decrease of the cross sections with increasing energy. In our isobar model this would be given by the W^2 dependence of the quasi-two-body form factors. According to vector dominance ideas these form factors are expected to be dominated either by the classical ρ, ω and ϕ mesons [2,3] , or by these in conjunction with further heavy vector mesons ($\rho'(1250)$, $\rho''(1600)$, etc.) [7] , or even continuum states [8]. The interference of different two-body intermediate states (e.g. $''\gamma'' \to \pi A_2 \to \rho\pi\pi$ *versus* $''\gamma'' \to \rho\epsilon \to \rho\pi\pi$) will be affected by these different hadronic contributions in the virtual photon channel. Nevertheless at fixed W our results are independent of such assumptions as long as we concentrate on only one particular two-body intermediate state.

Sect. 2 contains the relevant helicity formalism. In sect. 3 the calculations for the $\rho\pi\pi$ final state are given, in sect. 4 we present the results, and in sect. 5 the conclusions.

2. The helicity formalism for three-particle final states

We consider the reaction

$$e^+ + e^- \to h_1 + h_2 + h_3 , \tag{2.1}$$

where $p_\pm$, $\lambda_\pm$ are the momenta and helicities of the incoming leptons, p_i, λ_i the corresponding quantities for the outgoing hadrons h_1, h_2, h_3. In the one-photon-exchange approximation the scattering matrix elements are

$$T_{fi} = -\langle p_i, \lambda_i | J_\mu^{\mathrm{em}}(0)|0\rangle \frac{e}{W^2} \bar{v}_{\lambda_+}(p_+)\gamma^\mu u_{\lambda_-}(p_-), \tag{2.2}$$

where we use as state normalization

$$\langle p'\lambda'|p\lambda\rangle = (2\pi)^3 2p_0 \delta^{(3)}(p'-p)\delta_{\lambda\lambda'}. \tag{2.3}$$

$W = \sqrt{q^2}$ is the total energy in the center-of-mass system of the two leptons (= laboratory frame).

We take the laboratory Z-axis along the momentum p_+ of the positron and the z-axis of the decay system coordinate axes along the momentum p_1 of particle one. The orientation of the decay system with respect to the laboratory frame is given by the Euler angles α, β, γ (we use the convention of ref. [9] for these angles) and is shown in fig. 1.

The hadron system can now be described by the states

$$|\alpha\beta\gamma; E_i, \lambda_i\rangle = |p_i, \lambda_i\rangle, \tag{2.4}$$

where E_i are the hadron energies in the center-of-mass system. The Jacobian determinant of the transformation from one set of variables to the other is equal to one. From these states, states of definite angular momentum may be formed in the usual way [10]:

$$|JMK; E_i, \lambda_i\rangle = \int \mathrm{d}\alpha \, \mathrm{d}\cos\beta \, \mathrm{d}\gamma |\alpha\beta\gamma; E_i, \lambda_i\rangle D^{J\,*}_{MK}(\alpha, \beta, \gamma). \tag{2.5}$$

This state has total angular momentum J, component M along the laboratory Z-axis and component K along the decay system z-axis. The decomposition of the $|\alpha\beta\gamma; E_i, \lambda_i\rangle$ states in terms of states of definite angular momentum is given by the inverse of the above equation:

$$|\alpha\beta\gamma; E_i, \lambda_i\rangle = \sum_{J=0} \sum_{M,K=-J}^{J} |JMK; E_i, \lambda_i\rangle D^J_{MK}(\alpha, \beta, \gamma). \tag{2.6}$$

Since $J_\mu^{\mathrm{em}}(0)|0\rangle$ transforms as a state of angular momentum $J = 1$, the matrix element in eq. (2.2) is

$$J_M = \langle \alpha\beta\gamma; E_i, \lambda_i | J_M^{\mathrm{em}}(0)|0\rangle = \sum_{K=\pm,0} D^{1\,*}_{MK}(\alpha, \beta, \gamma) \Gamma_K^{\lambda_i}(E_i), \tag{2.7}$$

where J_M are the spherical components $J_\pm = \mp 1/\sqrt{2}\,(J_x \pm iJ_y)$, $J_0 = J_z$ and $\Gamma_K^{\lambda_i}(E_i)$ are the helicity coupling factors of the virtual photon to the hadrons defined by

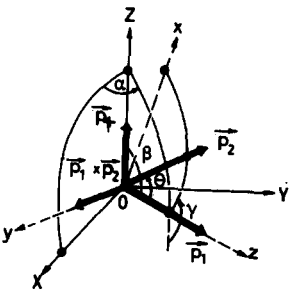

Fig. 1. Definition of Euler angles α, β, γ. The positron momentum is in the Z direction whereas p_1 and $p_1 \times p_2$ define the z and y axes.

$$\Gamma_K^{\lambda i}(E_i) = \langle 1, M, K; E_i, \lambda_i | J_M^{\mathrm{em}}(0) | 0 \rangle . \tag{2.8}$$

They are independent of M by rotational invariance. Conservation of parity leads to the constraints

$$\Gamma_K^{\lambda i}(E_i) = (-)^K \prod_{i=1}^{3} \eta_i (-)^{s_i - \lambda_i} \Gamma_K^{-\lambda i}(E_i) , \tag{2.9}$$

where η_i is the intrinsic parity of the ith particle and s_i is its spin. The cross section for $e^+e^- \to h_1 + h_2 + h_3$ is calculated from

$$\mathrm{d}^9\sigma = L^{\mu\nu} J_\mu J_\nu^* \frac{e^2}{2W^6(2\pi)^5} \delta^{(4)}(p_1 + p_2 + p_3 - p_+ - p_-) \frac{\mathrm{d}^3p_1\, \mathrm{d}^3p_2\, \mathrm{d}^3p_3}{8E_1E_2E_3} , \tag{2.10}$$

where

$$L_{\mu\nu} = p_{+\mu} p_{-\nu} + p_{-\mu} p_{+\nu} - \frac{W^2}{2} g_{\mu\nu} . \tag{2.11}$$

In the limit of vanishing lepton mass $L_{\mu\nu} = \frac{1}{2} W^2 \delta_{ij}$ for $i, j = 1,2$ and equal to zero otherwise. In this approximation the cross section expressed in spherical components of the current and after integration over d^3p_3 is:

$$\mathrm{d}^6\sigma = \frac{\alpha}{8W^4(2\pi)^4} \sum_{\text{spins}} \sum_{M=\pm} |J_M|^2 \, \delta((W - E_1 - E_2)^2 - m_\pi^2$$

$$- (p_1^2 + p_2^2 + 2|p_1||p_2| \cos\theta_{12})) \, \mathrm{d}\cos\theta_{12}\, \mathrm{d}\phi_{12}\, \mathrm{d}\cos\theta_1\, \mathrm{d}\phi_1\, \mathrm{d}E_1\, \mathrm{d}E_2 , \tag{2.12}$$

where ϕ_{12} and θ_{12} are the azimuthal and polar angles of p_2 with respect to p_1. The integration over $\cos\theta_{12}$ can easily be performed. Instead of the variables ϕ_{12}, θ_1 and ϕ_2 we shall go over to the variables α, β and γ defined previously and use the ex-

pansion (2.7) for J_M in terms of these new angular variables. Then we obtain for the differential cross section:

$$d^5\sigma = \frac{\alpha}{16W^4(2\pi)^4} \sum_{\lambda_i} \sum_{K,K'} \sum_{M=\pm} D^{1\,*}_{MK}(\alpha,\beta,\gamma)\, D^1_{MK'}(\alpha,\beta,\gamma)$$

$$\times \Gamma^{\lambda_i}_K(E_i)\, \Gamma^{\lambda_i *}_{K'}(E_i)\, d\alpha\, d\cos\beta\, d\gamma\, dE_1\, dE_2 \,. \tag{2.13}$$

(2.13) is the most general formula we can obtain for the differential cross section in the case of e^+e^- annihilation into three particles of arbitrary spin. We see that the angular distribution depends only on two angles β and γ (the dependence on α drops out) and on the helicity matrix elements $\Gamma^{\lambda_i}_K(E_i)$. The result (2.13) can be simplified further if we insert the explicit formulas for the D-functions

$$\frac{d^4\sigma}{d\cos\beta\, d\gamma/2\pi\, dE_1\, dE_2} = \frac{d^2\sigma_U}{dE_1\, dE_2} \tfrac{3}{8}(1+\cos^2\beta) + \frac{d^2\sigma_L}{dE_1\, dE_2} \tfrac{3}{4}\sin^2\beta$$

$$+ \frac{d^2\sigma_T}{dE_1\, dE_2} \tfrac{3}{4}\sin^2\beta\cos 2\gamma - \frac{d^2\sigma_I}{dE_1\, dE_2} \frac{3}{8\sqrt{2}} \sin 2\beta\cos\gamma \quad , \tag{2.14}$$

where

$$\frac{d^2\sigma_U}{dE_1\, dE_2} = \frac{\alpha}{12\, W^4(2\pi)^2} \sum_{\lambda_i} \sum_{K=\pm 1} |\Gamma^{\lambda_i}_K(E_i)|^2 \,,$$

$$\frac{d^2\sigma_L}{dE_1\, dE_2} = \frac{\alpha}{12\, W^4(2\pi)^2} \sum_{\lambda_i} |\Gamma^{\lambda_i}_0(E_i)|^2 \,, \tag{2.15}$$

$$\frac{d^2\sigma_T}{dE_1\, dE_2} = \frac{\alpha}{12\, W^4(2\pi)^2} \sum_{\lambda_i} \Gamma^{\lambda_i}_{+1}\, \Gamma^{\lambda_i *}_{-1} \,,$$

$$\frac{d^2\sigma_I}{dE_1\, dE_2} = \frac{\alpha}{12\, W^4(2\pi)^2} \sum_{\lambda_i} ((\Gamma^{\lambda_i}_{+1} - \Gamma^{\lambda_i}_{-1})\, \Gamma^{\lambda_i *}_0 + \text{c.c.}) \,.$$

$d\sigma_T$ is guaranteed to be a real quantity because of the constraints of parity conservation eq. (2.9). We see that by measuring the angular distribution in β and γ four independent cross sections σ_U, σ_L, σ_T, and σ_I can be determined. Here $d\sigma_U$ is the cross section for three particle production by an unpolarized transverse virtual

photon. $d\sigma_L$ is responsible for the production by a longitudinal virtual photon. $d\sigma_T$ describes the production by a transverse polarized virtual photon and $d\sigma_I$ comes from interference between transverse and longitudinal photons. The polarization is given with respect to the momentum p_1. Obviously the dependence of the cross section on β and γ is a consequence of the one-photon approximation. The cross section given in (2.13) can be integrated over the Dalitz plot. Then the following integrated angular distribution is obtained:

$$\frac{d^2\sigma}{d\cos\beta\, d\gamma/2\pi} = \sigma_U \tfrac{3}{8}(1+\cos^2\beta) + \sigma_L \tfrac{3}{4}\sin^2\beta$$

$$+ \sigma_T \tfrac{3}{4}\sin^2\beta\cos 2\gamma - \sigma_I \frac{3}{8\sqrt{2}}\sin 2\beta\cos\gamma\,. \tag{2.16}$$

The angle integrated Dalitz plot distribution is

$$\frac{d^2\sigma}{dE_1\, dE_2} = \frac{d^2\sigma_U}{dE_1\, dE_2} + \frac{d^2\sigma_L}{dE_1\, dE_2}\,, \tag{2.17}$$

and the total integrated cross section is

$$\sigma = \sigma_U + \sigma_L\,. \tag{2.18}$$

3. The process $e^+e^- \to \rho\pi\pi$

The kinematics for the virtual decay $\gamma \to \rho\pi_2\pi_3$ is given in fig. 2. We denote the momentum of the virtual photon by q and by p_1, p_2, p_3 the momenta of the three decay particles ρ, π_2 and π_3. Similarly as for two-body scattering processes it is useful to work with the Mandelstam invariants defined as

$$s = (q-p_1)^2 = W^2 + m_\rho^2 - 2WE_1\,,\quad t = (q-p_2)^2 = W^2 + m_\pi^2 - 2WE_2\,,$$

$$u = (q-p_3)^2 = W^2 + m_\pi^2 - 2WE_3\,.$$

Then we define the covariant tensor $T_{\mu\nu}$ by:

$$e^\mu(\lambda_1)^* T_{\mu\nu} = \langle p_1, \lambda_1; p_2; p_3 | J_\nu^{\mathrm{em}}(0)|0\rangle\,, \tag{3.2}$$

and expand $T_{\mu\nu}$ into gauge invariant covariants $F^i_{\mu\nu}$:

$$T_{\mu\nu} = \sum_{i=1}^{5} A_i(s,t)\, F^i_{\mu\nu}\,. \tag{3.3}$$

The covariants $F^i_{\mu\nu}$ are ($Q = p_2 - p_3$):

$$F^1_{\mu\nu} = (q p_1) g_{\mu\nu} - q_\mu p_{1\nu} ,$$

$$F^2_\mu = (q p_1) Q_\mu Q_\nu - (Q q) Q_\mu p_{1\nu} - (p_1 Q) q_\mu Q_\nu + (Qq\, Qp_1) g_{\mu\nu} ,$$

$$F^3_\mu = (q p_1) Q_\mu q_\nu - q^2 Q_\mu p_{1\nu} - (p_1 Q) q_\mu q_\nu + q^2 (p_1 Q) g_{\mu\nu} ,$$

$$F^4_\mu = (q p_1) p_{1\mu} Q_\nu - (q Q) p_{1\mu} p_{1\nu} - p_1^2 q_\mu Q_\nu + (q Q) p_1^2 g_{\mu\nu} ,$$

$$F^5_\mu = (q p_1) p_{1\mu} q_\mu - q^2 p_{1\mu} p_{1\nu} - p_1^2 q_\mu q_\nu + p_1^2 q^2 g_{\mu\nu} . \tag{3.4}$$

These covariants obey

$$F^i_{\mu\nu} q^\nu = 0 , \tag{3.5}$$

which is necessary because the electromagnetic current is divergenceless. Furthermore, to have complete symmetry between the electromagnetic current and the ρ meson we asked for

$$p_1^\mu F^i_{\mu\nu} = 0 , \tag{3.6}$$

which is advantageous for continuation in p_1^2 including $p_1^2 = 0$.

The helicity couplings we are interested in are obtained from

$$\Gamma^{\lambda_1}_K (E_1, E_2, E_3) = e^\mu (\lambda_1)^* T_{\mu\nu} e^\nu (K) , \tag{3.7}$$

if (3.7) is evaluated in the system $q = 0$ and the z-direction parallel to the ρ meson momentum p_1. Then with (3.3) the helicity form factors are related to the invariant amplitudes

$$\Gamma^{\lambda_1}_K (E_i) = \sum_{i=1}^{5} A_i (s, t, u) f^i_{\lambda_1 K} , \tag{3.8}$$

where

$$f^i_{\lambda_1 K} = e^\mu (\lambda_1)^* F^i_{\mu\nu} e^\nu (K) . \tag{3.9}$$

The $f^i_{\lambda_1 K}$ are listed in appendix A. This way we can study various exchange models without going through the calculation of the helicity matrix element for every new exchange contribution. We just specify the corresponding invariant amplitudes A_1, $A_2, \ldots, A_5$.

We investigate here a simple isobar model in order to see the effect of the finite widths of resonances and possible interferences in the s-, t- and u-channels.

Depending on the charge configuration of the final state ($\rho^0\pi^+\pi^-$, $\rho^0\pi^0\pi^0$ or $\rho^\pm\pi^\pm\pi^0$) we incorporate the ϵ resonance (0^{++}, $m_\epsilon = 0.7$ GeV, $\Gamma_\epsilon = 0.3$ GeV) in the s-channel, the π and ω poles and A_1 and A_2 resonances in the t- and u-channels (fig. 3). We remark that ϵ, A_1 and A_2 are in the physical region for $\gamma \to \rho\pi_2\pi_3$, whereas π and ω lie outside. Therefore π and ω constitute background terms to the resonance contributions.

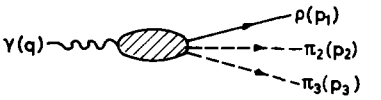

Fig. 2. Kinematic diagram for $\gamma \to \rho\pi\pi$.

In terms of the couplings which are defined in appendix B the contributions of the poles and resonances to the invariant amplitudes are calculated to be:

(a) Pion pole

$$A_1 = -g_{\rho\pi\pi}F_\pi(W^2)\left(\frac{1}{t-m_\pi^2}+\frac{1}{u-m_\pi^2}\right), A_2 = 2g_{\rho\pi\pi}F_\pi(W^2)\frac{1}{(t-m_\pi^2)(u-m_\pi^2)}, \tag{3.10}$$

$$A_3 = A_4 = A_5 = 0.$$

(b) Omega pole

$$A_1 = -\tfrac{1}{4}g_{\pi\omega\rho}g_{\pi\omega\gamma}(W^2)\,(2t+2m_\pi^2-\tfrac{1}{2}(s+m_\rho^2+W^2))\frac{1}{t-m_\omega^2}+(t\leftrightarrow u),$$

$$A_2 = A_5 = \tfrac{1}{4}g_{\pi\omega\rho}g_{\pi\omega\gamma}(W^2)\frac{1}{t-m_\omega^2}+(t\leftrightarrow u),$$

$$A_3 = A_4 = -\tfrac{1}{4}g_{\pi\omega\rho}g_{\pi\omega\gamma}(W^2)\frac{1}{t-m_\omega^2}-(t\leftrightarrow u). \tag{3.11}$$

For the resonance exchanges we include an energy dependent width in the Breit-Wigner formula, with the appropriate threshold factors [11] $(p/p_R)^{2l+1}$.

(c) ϵ resonance

$$A_1 = \frac{1}{s-m_\epsilon^2+im_\epsilon\Gamma_\epsilon(p(s)/p(m_\epsilon^2))}g_{\epsilon\pi\pi}(G^1_{\gamma\epsilon\rho}(W^2)-m_\rho^2W^2G^2_{\gamma\epsilon\rho}(W^2)),$$

$$A_5 = \frac{1}{s-m_\epsilon^2+im_\epsilon\Gamma_\epsilon(p(s)/p(m_\epsilon^2))}\tfrac{1}{2}(-s+m_\rho^2+W^2)g_{\epsilon\pi\pi}G^2_{\gamma\epsilon\rho}(W^2),$$

$$A_2 = A_3 = A_4 = 0, \tag{3.12}$$

where

$$p(s) = \tfrac{1}{2}(s-4m_\pi^2)^{\frac{1}{2}}, \tag{3.13}$$

is the momentum of the pion in the ϵ rest system off-mass-shell.

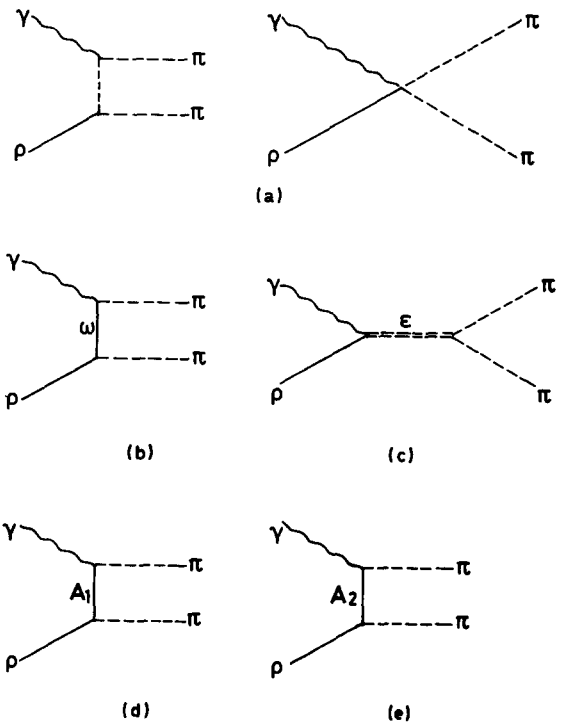

Fig. 3. Various exchange contributions to $\gamma \to \rho\pi\pi$.

(d) A_1 resonance

The formulas for the contribution of the A_1 meson in the t- and u-channel are much more complicated since both vertices consist of two independent terms with coupling constants $G^1_{\gamma A_1 \pi}(W^2)$ and $G^2_{\gamma A_1 \pi}(W^2)$ at the upper vertex and $G^1_{\rho A_1 \pi}$ and $G^2_{\rho A_1 \pi}$ at the lower vertex respectively (fig. 3d). We write down only the contribution of the t-pole. The u-pole term is obtained by the crossing rules (see for example (3.11) in connection with the ω-contribution). Then we have for the A_1 contribution to the invariant amplitudes

$$A_i = \frac{1}{t - m^2_{A_1} + i m_{A_1} \Gamma_{A_1}(p(t)/p(m^2_{A_1}))^3} \frac{a_i}{4}, \tag{3.14}$$

where the coefficients a_i are polynomials in t, i.e.

$$a_1 = h_1 \tfrac{1}{2}(4t - 4m^2_\pi + s + W^2 + m^2_\rho) - h_2(2W^2 m^2_\rho + \tfrac{1}{2}(t-u)(W^2 + m^2_\rho))$$
$$+ h_3 W^2 m^2_\rho K \tfrac{1}{2}(s - m^2_\rho - W^2),$$

$$a_2 = h_1 - h_2(W^2 + m_\rho^2) + h_3 W^2 m_\rho^2 K ,$$

$$a_3 = -h_1 - h_2(t - m_\rho^2 - m_\pi^2) + h_3 m_\rho^2 (t - m_\pi^2) K ,$$

$$a_4 = -h_1 - h_2(t - W^2 - m_\pi^2) + h_3 W^2 (t - m_\pi^2) K ,$$

$$a_5 = h_1 + 2 h_2 (t - m_\pi^2) + h_3 U K .$$

$p(t)$ is the momentum of the pion in the A_1 rest system:

$$p(t) = \frac{1}{2\sqrt{t}} \sqrt{\lambda(t, m_\rho^2, m_\pi^2)} , \tag{3.16}$$

and we used the following abreviations

$$K = m_{A_1}^4 - \tfrac{1}{2}(t + m_\rho^2 - m_\pi^2)(t + W^2 - m_\pi^2)(t - 2m_{A_1}^2) \frac{1}{s - w^2 - m_\rho^2} ,$$

$$U = 2 m_\rho^2 W^2 + (t - m_\pi^2)(t + 2 m_\rho^2 - m_\pi^2) ,$$

$$h_1 = G^1_{\gamma A_1 \pi}(W^2) G^1_{\rho A_1 \pi} ,$$

$$h_2 = \tfrac{1}{2} m_{A_1}^2 (G^1_{\gamma A_1 \pi}(W^2) G^2_{\rho A_1 \pi} + G^2_{\gamma A_1 \pi}(W^2) G^1_{\rho A_1 \pi}) ,$$

$$h_3 = G^2_{\gamma A_1 \pi}(W^2) G^2_{\rho A_1 \pi} . \tag{3.17}$$

(e) A_2 resonance

The contribution of the A_2 resonance is somewhat simpler in that there is only one coupling at the upper and lower vertex (fig. 3e) As in the A_1 case we give only the t-pole contribution. This can be written as follows:

$$A_i = \frac{1}{t - m_{A_2}^2 + i m_{A_2} \Gamma_{A_2} (p(t)/p(m_{A_2}^2))^5} G_{\gamma A_2 \pi}(W^2) G_{\rho A_2 \pi} b_i , \tag{3.18}$$

where

$$b_1 = \tfrac{1}{8} a(4t + 4m_\pi^2 - s - m_\rho^2 - W^2) + \tfrac{1}{2}(s - m_\rho^2 - W^2)(\tfrac{1}{4} b + \tfrac{1}{2} f + \tfrac{1}{2} e - c) ,$$

$$b_2 = -\tfrac{1}{8} a + \tfrac{1}{4} b , \; b_3 = \tfrac{1}{8} a - \tfrac{1}{4} b - \tfrac{1}{2} e , \; b_4 = \tfrac{1}{8} a - \tfrac{1}{4} b - \tfrac{1}{2} d , \; b_5 = -\tfrac{1}{8} a + \tfrac{1}{4} b + \tfrac{1}{2} f + \tfrac{1}{2} e - c , \tag{3.19}$$

and

$$a = \tfrac{1}{2}(s - m_\rho^2 - W^2) + \frac{1}{4 m_{A_2}^2}(t + W^2 - m_\pi^2)(t + m_\rho^2 - m_\pi^2) ,$$

$$b = \frac{1}{2(s-m_\rho^2-W^2)}\,\lambda(s, W^2, m_\rho^2)\,,$$

$$c = \frac{1}{s-m_\rho^2-W^2}\,((s-m_\rho^2-W^2)\,t + \tfrac{1}{2}(t + W^2-m_\pi^2)\,(t + m_\rho^2-m_\pi^2))\,,$$

$$d = \frac{1}{s-m_\rho^2-W^2}\,(W^2(t + m_\rho^2-m_\pi^2) + \tfrac{1}{2}(t + W^2-m_\pi^2)\,(s-m_\rho^2-W^2))\,,$$

$$e = \frac{1}{s-m_\rho^2-W^2}\,(m_\rho^2\,(t + W^2-m_\pi^2) + \tfrac{1}{2}(t + m_\rho^2-m_\pi^2)\,(s-m_\rho^2-W^2))\,,$$

$$f = \frac{1}{s-m_\rho^2-W^2}\,\tfrac{1}{2}(t + W^2-m_\pi^2)\,(s-m_\rho^2-3\,W^2)\,. \tag{3.20}$$

The decomposition of the cross section according to the polarization of the virtual photon, eq. (2.14), is a first step towards distinguishing the contributions of the various exchanges. For example in ϵ exchange, eq. (3.12), $A_2 = A_3 = A_4 = 0$ so that $\Gamma_-^+ = \Gamma_+^0 = \Gamma_0^+ = 0$ and therefore

$$\sigma_T = \sigma_I = 0\,. \tag{3.21}$$

The ϵ exchange diagram therefore contributes only to σ_U and σ_L. The angular distribution takes the simple form $\mathrm{d}\sigma/\mathrm{d}\cos\beta\,\mathrm{d}\gamma/2\pi \sim a + b\cos^2\beta$, independent of the azimuthal angle γ.

4. Results

We present in this section numerical results for the process $e^+e^- \to \rho\pi\pi$ using the isobar model of sect. 3. We exhibit the contributions of the various exchanges to the partial cross sections σ_U, σ_L, σ_T, σ_I which determine the integrated angular distribution of eq. (2.16). We also show the distributions on the Dalitz plot arising from the angle-integrated cross sections $\mathrm{d}^2\sigma/\mathrm{d}E_1\,\mathrm{d}E_2$, eq. (2.17) and the total integrated cross section eq. (2.18).

For the W dependence of the quasi-two-body from factors we use the simple VDM form:

$$G(W^2) = \frac{G(W^2=m_\rho^2)m_\rho^2}{f_\rho(W^2-m_\rho^2)}\,. \tag{4.1}$$

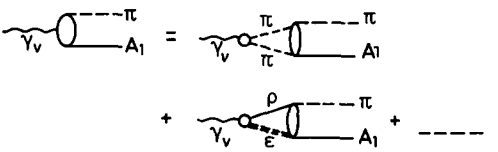

Fig. 4. Unitarity relation for the quasi-two-particle form factor $\gamma \to \pi A_1$.

For the energy range we consider here this may be a reasonable procedure, although for sufficiently high W we expect it to break down, as it does for large space-like values in the deep inelastic region. The pion and kaon form factors $G_{\gamma\pi\pi}(W^2)$ and $G_{\gamma K\bar{K}}(W^2)$, the only ones measured up to now in the time-like region [12], follow the VDM curve, at least as a first approximation, up to $W \approx 2$ or 3 GeV. This indicates that the heavier vector mesons such as the ρ', if they exist, couple weakly to the $\pi\pi$ channel [13]. Renard has considered the effect on these form factors of including higher vector mesons in the calculation, as well as the effects of inelastic intermediate state which contribute through unitarity [14]. It is clear that similar inelastic effects can contribute to the form factors which we are interested in, e.g. $\gamma \to \epsilon\rho \to \pi A_1$, see fig. 4. In this sense the assumption of eq. (4.1) means that we include only 2π intermediate states in the unitarity relation.

If such inelastic effects, or strongly coupled heavy vector mesons, were important in any of the channels which we are considering, their contributions would have to be added to that of the ρ meson, which is what we have calculated. Besides the W dependence this would affect the distributions at fixed W to the extent that the ρ' couples to the various channels with relative strengths different from the couplings of the ρ meson. Indeed, besides in the W dependence of the total cross section, which we shall show to be a rather insensitive test, it is in deviations from the distributions given here that the effect of the ρ' meson in e^+e^- annihilation should be searched for.

4.1. ϵ exchange

We consider first the ϵ exchange contribution of fig. 3c. As explained in sect. 3 an angular determination of the cross sections σ_U, σ_L, σ_T, σ_I will immediately show how important this contribution is: small values of σ_T, σ_I compared to σ_U, σ_L would indicate its dominance, appreciable values of σ_T, σ_I would point to the importance of other mechanisms.

The coupling of the ϵ to the $\rho\gamma$ channel involves two form factors; we use $G^1_{\epsilon\gamma\rho}(W^2)$, $G^2_{\epsilon\gamma\rho}(W^2)$ as defined in eq. (B.4). Whenever more than one form factor is involved in the coupling at any vertex the energy dependence of the cross section will depend on which form factors, corresponding to different possible covariant decompositions of the vertex function, are assumed to follow the "minimal" VDM prescription. We discuss this question more fully in connection with the A_1 exchange

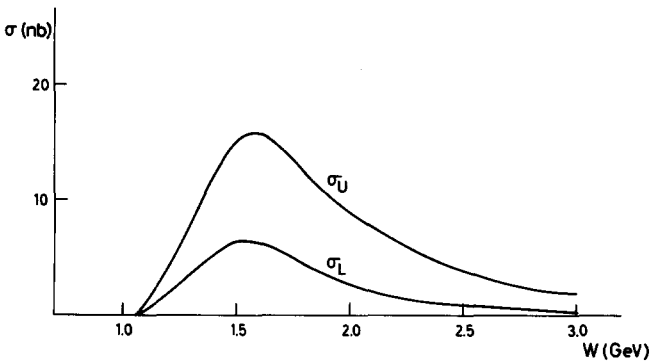

Fig. 5. Cross sections σ_U and σ_L for $e^+e^- \to \rho^0\pi^+\pi^- + \rho^0\pi^0\pi^0$ as a function of the total c.m. energy W for the ϵ exchange model with $G^2_{\epsilon\rho\gamma} = 0$.

contribution. Here we use VDM, eq. (4.1), for the form factor $G^1_{\epsilon\gamma\rho}(W^2)$, and set $G^2_{\epsilon\rho\gamma}(W^2) = 0$, as this leads to the sharpest decrease of the cross sections with energy, as favoured by the data.

We use throughout $f_\rho^2/4\pi = 2.26$; $m_\rho = 0.77$ GeV. For the ϵ meson we take $m_\epsilon = 0.7$ GeV, $\Gamma_\epsilon = 0.3$ GeV, and $G^1_{\epsilon\gamma\rho}(W^2 = m_\rho^2) = 38$ GeV^{-1}, as in ref. [15], and in agreement, through further application of VDM, with the estimates for $g_{\epsilon\gamma\gamma}$ of refs. [16, 17].

Fig. 5 shows σ_U and σ_L as functions of W. We see that σ_U dominates. σ_T and σ_I are identically zero. The effect of the finite-width correction inherent in the calculation with the three-particle final state is shown in fig. 6, where σ is compared to the result of the zero-width calculation with a two-particle final state [15]. We find that the two cross sections differ appreciably only in the threshold region; whereas in the two-body calculation the threshold is at $W = m_\rho + m_\epsilon$ and the cross

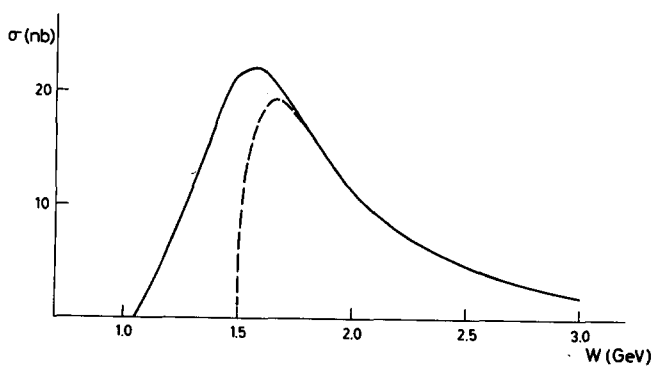

Fig. 6. Comparison of σ for ϵ-exchange contribution in zero-width approximation (two-body result) (dashed curve) with finite width calculation with $\Gamma = 0.3$ GeV (full curve).

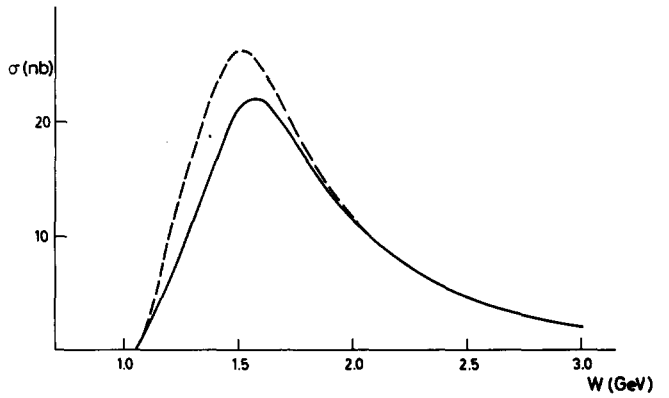

Fig. 7. Cross section σ for ϵ exchange (full curve) and for ϵ and π exchange (dashed curve) as a function of W.

section rises sharply above this point, in the new calculation the threshold is at $W = m_\rho + 2m_\pi$ and the cross section rises more gradually to its maximum. Above maximum the new calculation differs only little from the zerowidth approximation for this process.

4.2. ϵ and π exchange

In the calculation of the pion-exchange diagram of fig. 3a we use $g^2_{\rho\pi\pi}/4\pi = 2.86$. This diagram constitutes a background term to the resonant ϵ-exchange diagram in $e^+e^- \to \rho^0\pi^+\pi^-$. (In $e^+e^- \to \rho^0\pi^0\pi^0$ e.g. the background would be due to the ω-pole term.) It produces small but non-vanishing values of σ_T and σ_I. Its influence on σ is exhibited in fig. 7; it is seen to increase the cross section at maximum by roughly 10%, and thus produces a stronger fall-off of σ with W.

As mentioned in the introduction the Frascati data on $e^+e^- \to \pi^+\pi^-\pi^+\pi^-$ should be well described by consideration of the $\rho^0\pi^+\pi^-$ final state. The Frascati group further asserts that the scatter plot of the invariant masses $M(\pi_1\pi_2)$ *versus* $M(\pi_3\pi_4)$, as well as other kinematical evidence, strongly supports the assumption of a $\rho^0\epsilon^0$ intermediate state. It is therefore of interest to compare the result of our calculation of $e^+e^- \to \rho^0\pi^+\pi^-$ with ϵ and π exchange to the Frascati results. This comparison is shown in fig. 8. Here we have used a slightly different normalization compared to the case of pure ϵ exchange (fig. 6). The agreement is reasonable within the appreciable uncertainties present in this experiment. This does not mean that alternative interpretations of these data, for example in terms of strongly coupling heavy vector mesons [18] are not possible. We only wish to stress that the energy dependence of the total cross section is a rather insensitive test (note also our remarks concerning the ambiguity of the W behaviour corresponding to different choices of covariants). Consideration of more detailed distributions, such as those worked out in this paper, should lead to a clearer understanding of the dynamical mechanisms.

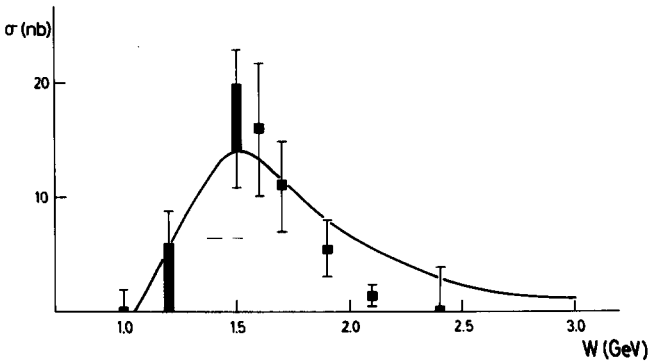

Fig. 8. Cross section σ ($\rho^0\pi^+\pi^-$) for ϵ and π exchange model compared with experimental data of ref. [5].

4.3. A_1 exchange

In attempting to calculate the contribution of the A_1 exchange diagram, fig. 3d, we are faced with the ambiguity concerning the form factors used for describing the $A_1\rho\pi$ vertex. One can use, for example, $G^1_{A_1\rho\pi}(W^2)$, $G^2_{A_1\rho\pi}(W^2)$ of eq. (B.4), or $F^1_{A_1\rho\pi}(W^2)$, $F^2_{A_1\rho\pi}(W^2)$ of eq. (B.7). As clearly shown by eq. (B.8) which relates the F and the G form factors, assuming VDM for the F form factors will lead to a W dependence of the G form factors different from that given by VDM,

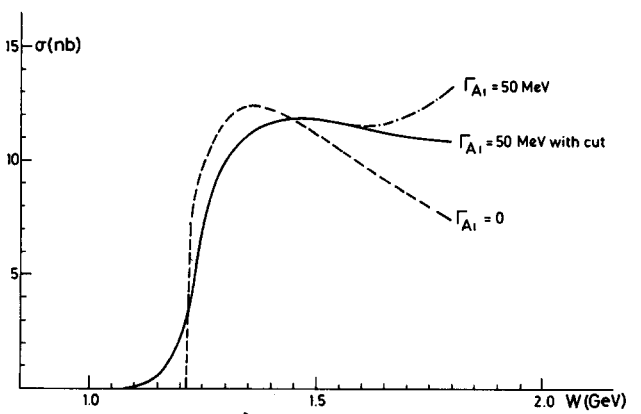

Fig. 9. Comparison of the contribution of A_1 exchange in the t-channel to σ in zero-width approximation (dashed curve) with finite width calculation with $\Gamma_{A_1} = 0.05$ GeV. Integrating over the Dalitz plot in the region of the A_1 resonance yields the full curve, integration of the complete Dalitz plot gives the dashed-dot curve.

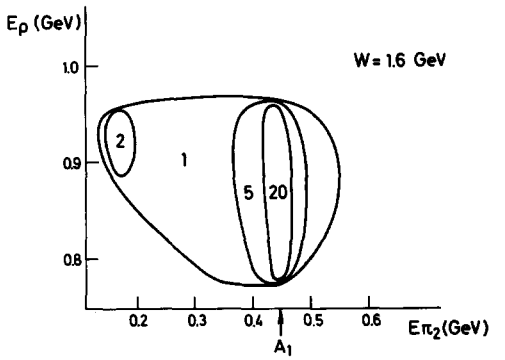

Fig. 10a. Dalitz plot for exchange mechanisms as in fig. 9 for $W = 1.6$ GeV.

eq. (4.1), and *vice versa*. For illustrative purposes we here use the VDM prescription for the F form factors, and set $F^1_{A_1\rho\pi}(W^2) = F^2_{A_1\rho\pi}(W^2)$ We take $m_{A_1} = 1.07$ GeV and $\Gamma_{A_1} = 0.05$ GeV.

Fig. 9 shows the total cross section resulting from A_1 exchange in the t-channel compared to the result of a zero-width two-body calculation. The finite-width corrections are seen to be more important here, at the higher energies as well as near threshold, than in the previous case. This follows from the higher spin of the exchanged system, and the resulting polynomial t-behaviour of the numerator of the propagator, eq. (3.14). At the pole position $t = m^2_{A_1}$ and in the narrow width approximation $\Gamma_{A_1} \to 0$ the expression for the cross section is identical to that of the two-body calculation. However as t takes on off-mass-shell values the numerator of the propagator changes, leading to a modified result after integration over the Dalitz plot. The effect increases at higher energies, as the phase space expands and

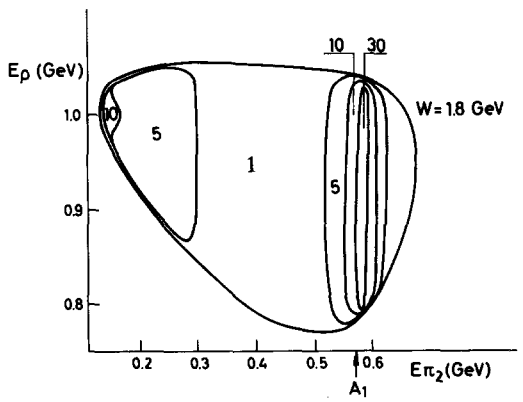

Fig. 10b. Dalitz plot for exchange mechanism as in fig. 9 for $W = 1.8$ GeV.

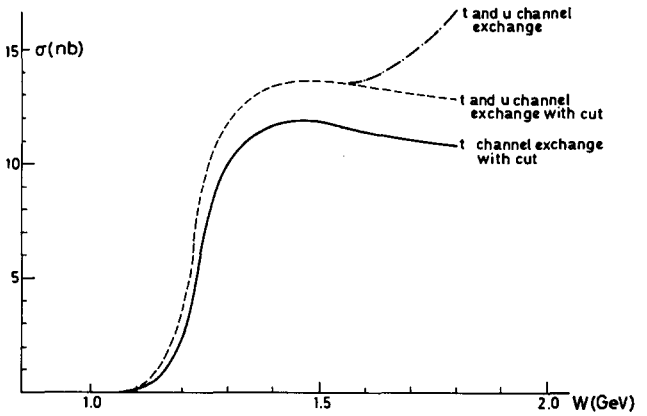

Fig. 11. σ for A_1 exchange in the t channel (full curve), t- and u-channel (dashed curve), t- and u-channel integrated over the complete Dalitz plot (dashed-dot curve).

the far regions of the Dalitz plot are even further removed from the resonance region. Above a certain energy the rising polynomial effect in the numerator of the propagator overcomes the damping effect of the Breit-Wigner denominator, and in the integration one begins to pick up significant contributions from regions of the Dalitz plot which are not in the vicinity of the resonance. In the present process this phenomenon shows up as an enhancement in the upper left hand corner of the Dalitz plot, which, as seen in figs. 10a and 10b, sets in rather abruptly at $W \approx 1.6$ GeV. Whether this enhancement should be considered physical, or whether it arises from the inadequacy of using the simple Feynman-graph prescription in kinematical

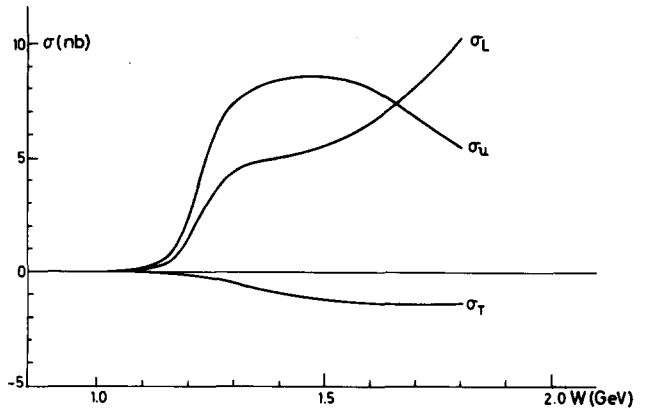

Fig. 12. Cross sections σ_U, σ_L and σ_T for A_1 exchange in the t- and u-channel integrated over the complete Dalitz plot. $\sigma_I \approx 0$.

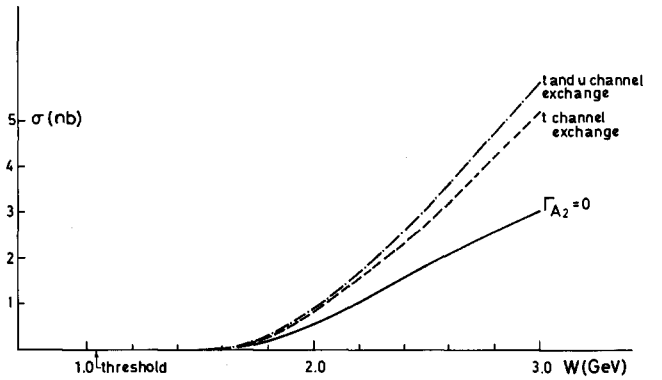

Fig. 13. σ for A_2 exchange in the t channel (dashed curve), t- and u-channel (dashed-dot curve) and for zero-width approcimation (full curve).

regions so far removed from the resonance pole, is unclear. A better method might be to allow for the reggeization of the exchanged particle off-mass-shell, and the subsequently modified behaviour of the propagator. We have not attempted here any such refinements. We merely note that the onset of the effect is clearly indicated in the Dalitz plots, it is clearly separated in phase-space from the resonance region, and in the full curve in fig. 9 we have simply subtracted it by hand from the total cross section. In the case of A_2 exchange the still higher spin and the correspondingly stronger damping effect of the $(p/p_R)^{2l+1}$ factor in the Breit-Wigner denominator cancel this effect entirely.

The A_1 exchange contributes in both the t- and u-channels, and when we include both in the calculation we find that interference between the two channels gives rise to an approximately 10–15% effect in the total cross section (fig. 11).

Fig. 12 shows the separation of the cross section according to the polarization state

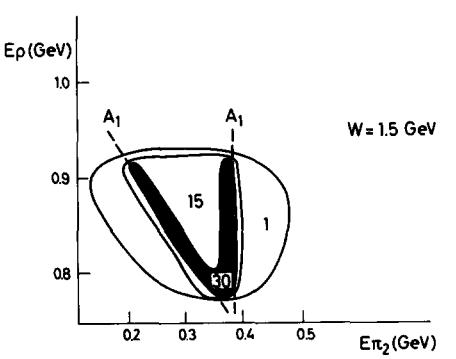

Fig. 14. Dalitz plot for A_1 exchange at $W = 1.5$ GeV.

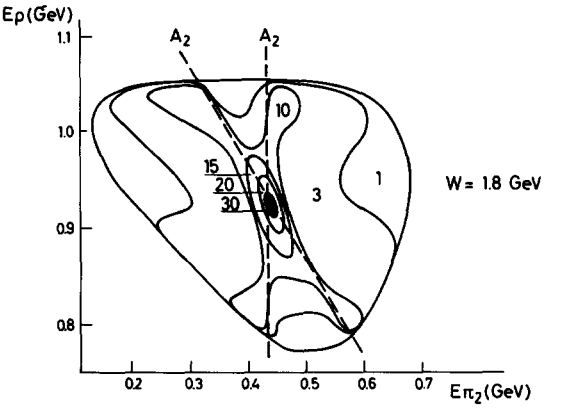

Fig. 15. Dalitz plot for A_2 exchange at $W = 1.8$ GeV.

of the virtual photon. We see that here σ_U and σ_L are of comparable magnitude. The rise at high energies due to the numerator effect mentioned previously occurs only in σ_L.

4.4. A_2 exchange

Fig. 13 shows the total cross section resulting from A_2 exchange, with m_{A_2} = = 1.31 GeV, $\Gamma_{A_2} = 0.076$ GeV. Although as mentioned before the factor $(p/p_R)^{2l+1}$ in the Breit-Wigner denominator cancels the effect of the rising numerator far from the resonance pole, the high spin nevertheless causes this variation to be of importance in the pole vicinity, and the finite-width corrections are correspondingly larger than in the previous cases. We also show here the effect of t- and u-channel interference. We see that with the couplings we have used the contribution of this mechanism is much smaller than that of those previously considered in the energy range of interest.

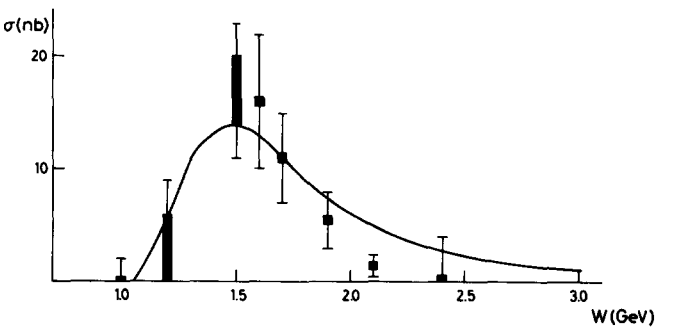

Fig. 16. $\sigma(\rho^0\pi^+\pi^-)$ for $\pi + \epsilon + A_1$ model compared to data of ref. [5].

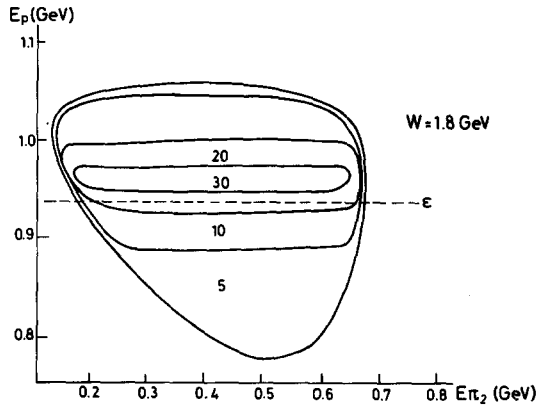

Fig. 17a. Dalitz plot for pure ϵ exchange at $W = 1.8$ GeV.

4.5. Comparison of various exchange mechanisms

Clearly interferences of t- and u-channel contributions corresponding to a specific exchange and interferences of different resonance contributions are much more prominent in the Dalitz plot distribution than in σ_{tot}. The previous figs. 11 and 13 show the effect of the t-u channel interference for A_1 and A_2 exchange. Figs. 14 and 15 exhibit this effect in the Dalitz plot distributions. Fig. 14, the Dalitz plot for A_1 exchange at $W = 1.5$ GeV, is a case where the resonance bands intersect outside the physical region below the lower boundary. Even in this case we see an enhancement in the overlap region of the resonance bands. For increasing W the bands emigrate towards the boundaries so that the intersection moves further away from the physical region (see (3.1) for the locations of the two bands in the E_1, E_2 plot).

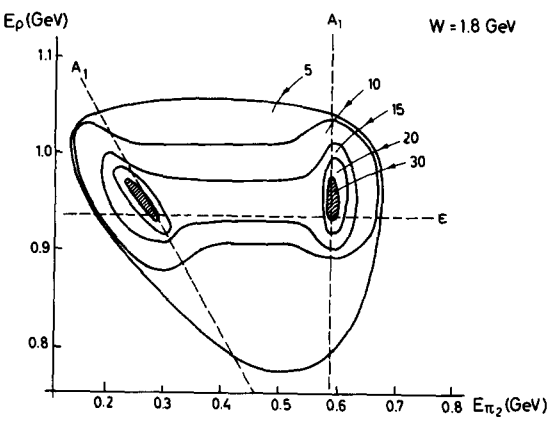

Fig. 17b. Dalitz plot for $\pi + \epsilon + A_1$ model at $W = 1.8$ GeV.

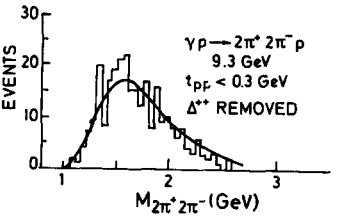

Fig. 18. Comparison of four pion mass spectrum is $\gamma p \to \pi^+\pi^-\pi^+\pi^- p$ [20] with $\epsilon + \pi$ exchange model.

For A_2 exchange at $W = 1.8$ GeV the intersection of the resonance bands is at the center of the Dalitz plot (fig. 15). With increasing W one obtains a plot similar to fig. 14 (for the A_1 case).

To see the effect of interference between different resonances we have calculated the cross section due to combined π, ϵ and A_1 exchange (with $G^2_{\pi A_1 \gamma} = 0$). Fig. 16 gives σ for $e^+e^- \to \rho^0\pi^+\pi^-$ as a function of W. Comparing this to fig. 8 we see that the addition of A_1 exchange with $G^2_{\pi A_1 \gamma} = 0$ and $\Gamma_{A_1} = 0.050$ GeV modifies σ only slightly near threshold. However as we see in fig. 17a, b the A_1 contribution shows up clearly in the Dalitz plot.

5. Conclusions

In this paper we have presented the general formalism for quasi-three-particle production in e^+e^- collisions. In the one-photon exchange approximation the cross section is given as sum of four terms σ_U, σ_L, σ_T, σ_I which have a simple interpretation in terms of the polarization states of the virtual photon along the z-axis of the decay system (in our case along the momentum of one of the outgoing particles). This is analogous to the familiar decomposition of the electroproduction cross section. The dynamical information is contained in helicity amplitudes which can be partially disentangled by determining the cross sections σ_U, σ_L, σ_T and σ_I. In order to obtain further dynamical information it would be necessary to consider the polarization of the final state particles and/or of the incoming beams [4].

For the particular final state $\rho\pi\pi$ we have calculated various distributions of experimental interest. When empirical data are available this should be of help to distinguish possible dynamical mechanisms.

In the energy range from threshold to $W \approx 3$ GeV it is possible that the cross section is dominated by resonances which can couple to the various channels. In this spirit we have considered the contributions of ϵ exchange in the s channel, A_1 and A_2 exchange in the t- and u-channels as well as the background terms arising from exchange of the stable particles π and ω.

We find that a reasonable interpretation of the Frascati data for $e^+e^- \to \pi^+\pi^-\pi^+\pi^-$

can be achieved by assuming the dominance of the ϵ exchange diagram and using the naive ρ dominance model for the coupling of the photon to hadrons. We can give a similar interpretation to the four pion enhancement in the photoproduction process $\gamma p \to \pi^+\pi^-\pi^+\pi^- p$, observed at SLAC [19]. This is shown in fig. 18. Thus the experiments which are taken as the evidence for the existence of a heavy vector meson $\rho'(1600)$, coupling directly to the photon, can be as well understood without invoking any new particle. One should note that in our interpretation the $\rho\epsilon$ electromagnetic form factor is dominantly real in the W range considered whereas the existence of a ρ' would give a dominantly imaginary form factor.

It has been claimed in the literature [20] that our interpretation of the four pion enhancement is refuted by an experiment of Eisenberg et al. which looked for a similar signal in the reaction $\pi^+ p \to \rho^0\pi^+\pi^-\Delta^{++}$. Unfortunately their conclusion depends on an *ad hoc* background subtraction. With another background curve their results could as well be compatible with the expected event rate from the ρ tail.

Appendix A

Here we list the transformation coefficients $f^i_{\lambda_1 K}$, defined in (3.9), which relate the helicity decay matrix elements to the invariant amplitudes $A_i(s,t)$ (see (3.8)):

$$
\begin{aligned}
f^1_{++} &= -(qp_1)\,,\\
f^2_{++} &= -2(qp_1)\boldsymbol{p}_2^2\sin^2\theta - (Qp)\,(Qp_1)\,,\\
f^3_{++} &= -W^2(p_1Q)\,,\\
f^4_{++} &= -(Qq)\,m_\rho^2\,,\\
f^5_{++} &= -W^2 m_\rho^2\,;
\end{aligned}
\qquad \text{(A.1)}
$$

$$
\begin{aligned}
f^1_{+-} &= f^3_{+-} = f^4_{+-} = f^5_{+-} = 0\,,\\
f^2_{+-} &= -2(qp_1)\,\boldsymbol{p}_2^2\sin^2\theta\,;
\end{aligned}
$$

$$
\begin{aligned}
f^1_{0+} &= f^3_{0+} = f^5_{0+} = f^5_{0+} = 0\,,\\
f^2_{0+} &= (qp_1)/m_\rho\,(|\boldsymbol{p}_1|Q_0 - E_1\,(|\boldsymbol{p}_1| + 2|\boldsymbol{p}_2|\cos\theta)\sqrt{2}|\boldsymbol{p}_2|\sin\theta\\
&\quad -(p_1Q)|\boldsymbol{p}_1|\,q_0\sqrt{2}\,|\boldsymbol{p}_2|\sin\theta/m_\rho\,,\\
f^4_{0+} &= -\sqrt{2}\,m_\rho\,|\boldsymbol{p}_1|q_0\,|\boldsymbol{p}_2|\sin\theta\,;
\end{aligned}
$$

$$f^1_{+0} = f^3_{+0} = f^4_{+0} = f^5_{+0} = 0\,,$$

$$f^2_{+0} = -(qp_1)\sqrt{2}\,|p_2|\sin\theta\,(2|p_2|\cos\theta + |p_1|) + Qp\sqrt{2}\,|p_1|\,|p_2|\sin\theta\,,$$

$$f^3_{+0} = W^2\sqrt{2}\,|p_1|\,|p_2|\sin\theta\,;$$

$$f^1_{00} = -q_0 m_\rho\,,$$

$$f^2_{00} = \{-(qp_1)\,(|p_1|\,Q_0 - E_1\,(|p_1| + 2|p_2|\cos\theta)\,(2|p_2|\cos\theta + |p_1|)$$

$$+ (qQ)\,(|p_1|\,Q_0 - E_1\,(|p_1| + 2|p_2|\cos\theta))\,|p_1|$$

$$+ (p_1 Q)\,|p_1|\,q_0(2|p_2|\cos\theta + |p_1|) - (Qp)\,(Qp_1)\,E_1\}/m_\rho\,,$$

$$f^3_{00} = W^2/m_\rho\,(|p_1|\,Q_0 - E_1\,(|p_1| + 2|p_2|\cos\theta)\,|p_1| - (Qp_1)E_1)\,,$$

$$f^4_{00} = m_\rho\,|p_1|\,q_0\,(2|p_2|\cos\theta + |p_1|) - (Qq)\,m_\rho E_1\,,$$

$$f^5_{00} = -m_\rho W^2 E_1\,.$$

In these formulas θ is the angle between p_1 and p_2 and is given by (see (2.12)):

$$\cos\theta = \frac{1}{2|p_1||p_2|}\,(W - E_1 - E_2)^2 - m_\pi^2 - p_1^2 - p_2^2)\,. \tag{A.2}$$

Appendix B

In this appendix we collect the definitions of the various couplings which are needed to calculate the diagrams in fig. 3a–3f. We start with the couplings of mesons to the photon. They are:

$$\langle \pi^+(p_a), \pi^-(p_b)\,|J_\mu(0)|0\rangle = (p_a - p_b)_\mu\,F_\pi(W^2)\,, \tag{B.1}$$

$$\langle \pi^0(p_a), \omega(p_b, \gamma)|J_\mu(0)|0\rangle = i\,\epsilon_{\mu\alpha\beta\gamma}\,p_a^\alpha p_b^\beta\,F_{\pi\omega\gamma}(W^2)\,, \tag{B.2}$$

$$\langle \pi^+(p_a), A_2^-(p_b, \gamma_1, \gamma_2)|J_\mu(0)|0\rangle = i\,\epsilon_{\mu\alpha\beta\gamma_1}\,p_a^\alpha q^\beta\,p_{a\gamma_2}\,F_{\pi A_2\gamma}(W^2)\,. \tag{B.3}$$

In (B.2) the index γ stands for the polarization of the ω whereas in (B.3) γ_1 and γ_2 are the tensor indices which multiply the polarization vector of A_2. In the cases $\gamma \to \pi\pi$, $\pi\omega$ and πA_2 we have only one independent form factor. This is not the case for $\gamma \to \pi A_1$, where we have two independent form factors. We used the following decomposition:

$$\langle \pi^+(p_a), A_1^-(p_b, \nu)|J_\mu(0)|0\rangle = G^1_{\pi A_1 \gamma}(W^2)\,((p_b q)g_{\mu\nu} - p_{b\mu}q_\nu)$$
$$+ G^2_{\pi A_1 \gamma}(W^2)\,(p_b q)\,((p_b q)q_\mu p_{b\nu} - W^2 p_{b\mu}p_{b\nu}) - m^2_{A_1}((p_b q)q_\mu q_\nu - W^2 p_{b\mu}p_{b\nu}))\,. \tag{B.4}$$

The decomposition (B.4) obeys

$$q^\mu \langle \pi^+(p_a) A_1^-(p_b, \nu)|J_\mu(0)|0\rangle = 0\,, \tag{B.5}$$

but also

$$p_b^\nu \langle \pi^+(p_a), A_1^-(p_b, \nu)|J_\mu(0)|0\rangle = 0\,, \tag{B.6}$$

where ν stands for the polarization component of the A_1 meson. In ref. [15] a different definition for πA_1 transition form factors was introduced. This is the following:

$$\langle \pi^+(p_a), A_1(p_b, \nu)|J_\mu(0)|0\rangle = (F^1_{\pi A_1 \gamma}(W^2) + F^2_{\pi A_1 \gamma}(W^2))$$
$$\times (g_{\mu\nu}q^2 - q_\mu q_\nu) - F^2_{\pi A_1 \gamma}(W^2)\,(g_{\mu\nu}(qp_b) - p_{b\mu}q_\nu)\,. \tag{B.7}$$

The decomposition (B.7) does not obey (B.6). The relation between the form factors G^1 and G^2 and F^1 and F^2 is:

$$G^1(qp_b) = (F^1 + F^2)\,q^2 - F^2(qp_b)\,,$$
$$G^2 m^2_{A_1}(qp_b) = F^1 + F^2\,. \tag{B.8}$$

The same couplings (B.4) and (B.7) are used for $\gamma \to \epsilon\rho$ where π and A_1 in (B.4) and (B.7) are replaced by the labels ϵ and ρ.

It is clear that the same definitions (B.1) to (B.8) can be used for the coupling of the ρ to $\pi\pi$, $\pi\omega$, πA_2, πA_1 and $\epsilon\rho$. The form factors F_π, $F_{\pi\omega\gamma}$ etc. in (B.1) to (B.8) are replaced by appropriate coupling constants $g_{\rho\pi\pi}$, $F_{\omega\rho}$, $F_{\pi A_2 \rho}$, $G^i_{\pi A_1 \rho}$ and $G^i_{\epsilon\rho\rho}$.

The coupling constant of the ϵ to $\pi\pi$ is defined by

$$\langle \pi^+, \pi^-|J_e(0)|0\rangle = g_{\epsilon\pi\pi}\,. \tag{B.9}$$

References

[1] Orsay results:
I. Le Francois, Proc. of the 1971 Int. Symposium on electron and photon interactions at high energies, Cornell University Ithaca N.Y., Aug. 23–27, 1971.
Frascati results:
$\gamma\gamma$ group:
C. Bacci et al., Phys. Letters 38B (1972) 551; 44B (1973) 533;

$\mu\pi$ group:
G. Barbanio et al., Nuovo Cimento Letters, 3 (1972) 689;
B. Borgia et al., Nuovo Cimento 13A (1973) 593;
F. Ceradini et al., Phys. Letters 43B (1973) 341.
Boson group:
B. Bartoli et al., Phys. Rev. D6 (1972) 2374.
CEA results:
A. Litke et al., Phys. Rev. Letters 30 (1973) 1189.
K. Strauch, Proc. of the Int. Symposium on electron and photon interactions at high energies Bonn, Aug. 27–31, 1973.

[2] G. Kramer, J.L. Uretsky and T.F. Walsh, Phys. Rev. D3 (1971) 719;
L. Layssac and F.M. Renard, Nuovo Cimento Letters 1 (1971) 197; Nuovo Cimento 6 1971 134;
A.M. Altukhov and I.B. Khriplovich, Sov. J. Nucl. Phys. 13 (1971) 352;
G. Kramer, 1972 CERN School Lectures, Grado, May 1972.

[3] G. Kramer and T.F. Walsh, DESY report, DESY 72/46; Z. Phys. 263 (1973) 361;
K. Schilling, Nuovo Cimento 16A (1973) 217.

[4] N.M. Avram and D.H. Schiller, University of Timisoara preprint F.T. 1/73 (April 1973); DESY 73/47; Nucl. Phys. B70 (1974) 272.

[5] F. Cerandini et al., Phys. Letters 43B (1973) 341.

[6] R. Jackiw and G. Preparata, Phys. Rev. Letters 22 (1969) 975;
N. Cabibbo, G. Parisi and M. Testa, Nuovo Cimento Letters 4 (1970) 35;
S.D. Drell, D.J. Levy and T-M. Yan, Phys. Rev. D1 (1970) 1617;
R.V. Landshoff and J.C. Polkinghorne, Phys. Reports 5 (1972) 1;
N.S. Craigie, A.G. Kraemmer and K.D. Rothe, Nuovo Cimento 11A (1972) 645, 665;
Z. Phys. 259 (1973) 1;
R. Gatto and G. Preparata, DESY report, DESY 73/15 (May 1973);
J. Engels, K. Schilling and H. Satz, Nuovo Cimento 17A (1973) 535.

[7] A. Bramon, E. Etim and M. Greco, Phys. Letters 41B (1972) 609;
M. Greco, Nucl. Phys. B63 (1973) 398.

[8] J.J. Sakurai and D. Schildknecht, Phys. Letters 40B (1972 121; 41B (1972) 489; 42B (1972) 216.

[9] M.E. Rose, Elementary theory of angular momentum (Wiley New York, 1957).

[10] S.M. Berman and M. Jacob, Phys. Rev. 139 (1965) B 1023;
J. Werle, Nucl. Phys. 44 (1963) 579, 637; Relativistic theory of reactions (North-Holland, Amsterdam, 1966).

[11] J.D. Jackson, Nuovo Cimento 34 (1964) 1644.

[12] M. Bernardini et al., Phys. Letters 46B (1973) 261.

[13] B. Hyams et al., $\pi\pi$ phase-shift analysis from 600 to 1900 MeV, preprint MPI-PAE/Exp E1. 28, Max-Planck-Institut fur Physik und Astrophysik, München.

[14] F.M. Renard, Phys. Letters 47B (1973) 361;
G. Bonneau and F. Martini, Nuovo Cimento 13A (1973) 413.

[15] G. Kramer and T.F. Walsh, see ref. [3].

[16] B. Schrempp-Otto, F. Schrempp and T.F. Walsh, Phys. Letters 36B (1971) 463;
J. Baacke, T.H. Chang and H. Kleinert, Nuovo Cimento 12A (1972) 21.

[17] G. Schierholz and K. Sundermeyer, Nucl. Phys. B40 (1972) 125.

[18] A. Bramon and M. Greco, Nuovo Cimento Letters 3 (1972) 693;
K. Fujikawa and P.J. O'Donnell, Phys. Rev. D8 (1973) 3994;
M. Böhm, H. Joos and M. Krammer, DESY report, DESY 73/20 (1973).

[19] SLAC-Berkeley-Tufts Collaboration, H.H. Bingham et al., Phys. Letters B41 (1972) 635
G. Smadja et al., Experimental meson spectroscopy – 1972, ed. A.H. Rosenfeld and K. Lai;
T. Ferbel and P. Slattery, University of Rochester preprint COO-3065-40.
[20] Y. Eisenberg et al., Phys. Letters B43 (1973) 149;
K.C. Moffeit, Rapporteurs talk at the Bonn Conf. 1973.